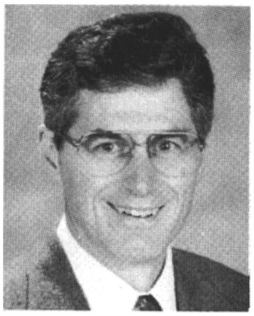

Tom Milligan
Assoc. Editor,
Antenna Designer's Notebook
8204 West Polk Place
Littleton, CO 80123 USA
Tel: +1 (303) 977 7268
Fax: +1 (303) 977 8853
E-mail: TMilligan@ieee.org

Broadband and Dual-Band Coplanar Folded-Slot Antennas (CFSAs)

Ahmad A. Gheethan and Dimitris E. Anagnostou

South Dakota School of Mines and Technology
Rapid City, SD 57701, USA
Tel: +1 (605) 394-4184; Fax: +1 (605) 394-2913; E-mail: danagn@ieee.org

Abstract

This paper presents a unified design methodology for dual-band and broadband coplanar folded-slot antennas (CFSAs). The design is achieved by using a coplanar waveguide-fed antenna element that is asymmetric with respect to the folded slot, and by adjusting the length of the stub inside the slot. A mathematical derivation, based on a transmission-line model for the asymmetrically-fed coplanar folded-slot antenna, is used on a single-frequency coplanar folded-slot antenna to determine the condition for a second resonance. In this way, when the second resonant frequency is close to the first, broadband uniplanar antennas with ~30% bandwidth can be designed. In addition, at the dual-band mode, a frequency ratio (f_2/f_1) of the order of 2.5 or more can be obtained. The effect of the ratio of the feed-shift distance to the length of the stub on the bandwidth is an important parameter, and is shown for both the broadband and dual-band designs. The presented method and tables are simple to use, provide very accurate results, and correctly predict the resonant frequencies for the dual-band coplanar folded-slot antennas. The theoretical and simulated results were verified by measurements of fabricated prototypes. The design guidelines cover a broad range of applications in the 2.4 GHz to 5.25 GHz range, with various bands and bandwidths.

Keywords: Coplanar folded slot antenna; slot antennas; coplanar transmission lines; coplanar waveguides; dual-band antennas; asymmetric feeding; broadband antennas

1. Introduction and Related Literature

Coplanar folded-slot antennas (CFSAs) are of interest due to their typically broader bandwidth (relative to other resonant planar antennas, like dipoles), and due to their broadside dipole-like radiation patterns [1]. Weller et al. [1] described the design of coplanar folded-slot antennas. They consist of a folded slot with a circumference (which, for dual-band coplanar folded-slot antennas, will later be defined as the *outer* circumference, instead of the *mean* [1]) that is approximately equal to one guided wavelength (λ_g). They can be fed with a coplanar waveguide (CPW) or a finite-ground coplanar (FGC) line from one end, allowing for easy integration with other components, three-terminal devices, or MMICs for microwave amplification and reception [2-6]. These antennas can be conformed to curved surfaces [7], and can cover holes or gaps of irregularly shaped structures. All of these characteristics make such antennas widely popular for many microwave applications. In addition, their resonant frequencies and patterns are relatively independent from temperature variations, making them excellent candidates for high-temperature sensor applications [8]. Recently, reconfigurable coplanar folded-slot antenna designs were reported [9, 10]. In [9], a coplanar folded-slot antenna with ferroelectric materials was

tuned, while in [10] a coplanar folded-slot antenna with PIN diodes was reconfigured and this altered its resonant frequency.

For efficient matching, in [11] a method of increasing the slot width (W_a) away from the feed was described. Also, bandwidths as broad as 44% and 80% have been achieved by modifying the shape of the slot [12]. Dual-band coplanar folded-slot antennas were realized in [13] by using double slots, and in [14] by using a T-matching network. However, no unified approach for the design of both broadband and dual-band coplanar folded-slot antennas exists in the literature. In addition, most design procedures involve a parametric study of the shape of the slot, and provide little insight into the understanding of the antenna's functionality and design.

Here, we present a unified approach, based on analytical equations for the design of broadband *and* dual-band coplanar folded-slot antennas. Both broadband and dual-band designs are achieved using a single off-center feed (relative to the center of the folded slot), and by adjusting the length of the stub element that is inside the antenna's aperture. With this method, a second resonance is added to the antenna's response, without the need for further modification or reconfiguration of the circumference of the folded slot. This asymmetric feeding has been used in the past to match stacked-patch antennas fed through a resonant slot [15], and to achieve broad bandwidth and dual-bandwidth with traditional (not folded) slot antennas [16].

First, the off-center-fed coplanar folded-slot antenna is studied, through an equivalent transmission-line model that is introduced. The model helps in deriving the condition for achieving the second resonant frequency, and provides physical insight into the antenna's operation at each mode. The effect of the off-center feed on the return loss is determined through a parametric study, and the conditions for good matching are extracted. Broadband and dual-band prototypes are designed using the proposed method to validate our study. Measurements show good agreement with calculations and simulations. The design steps for broadband and dual-band off-center-fed coplanar folded-slot antennas are summarized in the last section.

2. Off-Center-Fed Coplanar Folded-Slot Antennas

2.1 The Condition for Second Resonance of Off-Center-Fed Coplanar Folded-Slot Antennas and their Design Procedure

The center-fed and off-center-fed schematics of a coplanar folded-slot antenna are shown in Figures 1a and 1b. A traditional center-fed reference coplanar folded-slot antenna with a single resonance at 2.4 GHz was first designed and matched according to [1, 11], by making the outer circumference of the slot equal to one wavelength, λ_g. The substrate used was a 32 mil (0.8128 mm) RO4003C laminate, with a relative permittivity of 3.55, and 1 oz copper [17].

This asymmetrically fed antenna can be considered to consist of two open-circuited transmission-line sections of different lengths (due to the off-center feed). Its transmission-line equivalent circuit model was then extracted based on [18], and this is shown in Figure 1c. This model ignores the capacitance at the discontinuity between the ends of the open stub and the ground plane. However, this capacitance is small (in the femtofarad (fF) range, [19]) and does not affect the model's accuracy.

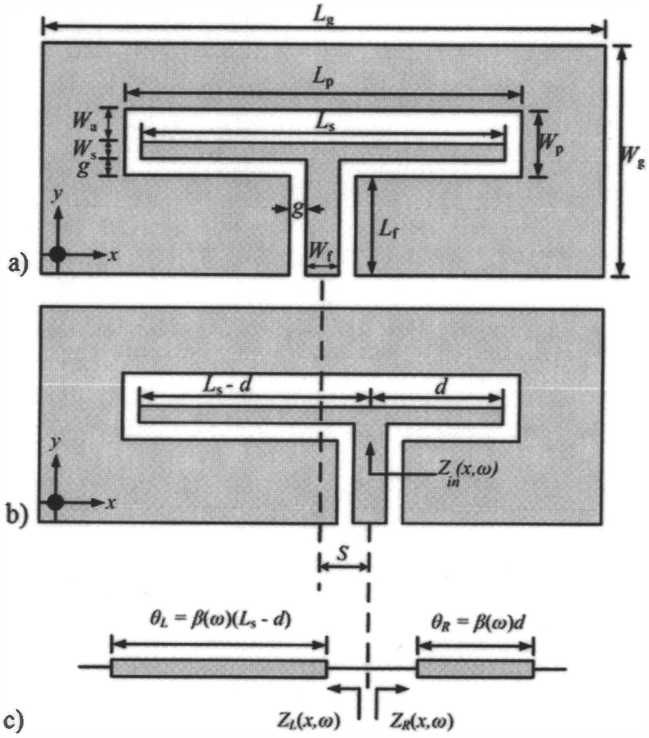

Figure 1. Schematics of the coplanar folded-slot antenna: (a) traditional, center-fed; (b) off-center fed; and (c) the transmission-line model for the off-center coplanar folded-slot antenna. The size of the slot, the size of the ground plane, and the antenna dimensions are the same in both schematics (a) and (b).

To specify the second resonant frequency of the asymmetric coplanar folded-slot antenna, we applied the transverse-resonance technique [20] to the transmission-line model of the antenna, along the length of its x axis. This technique has been applied in the past in other planar and conformal antennas, for example, as in [21], where it was applied in the design of reconfigurable slot antennas with excellent accuracy. Here, it was applied to the structure in Figure 1b at the terminals of the slot, at the junction where the 50 Ω coplanar-waveguide feed line splits into the two open-circuited stubs, which each present a purely imaginary impedance (reactance). The right and left input impedances are functions of x (the offset variable) and of ω. The transverse-resonant technique [20] states that

$$Z_L(x') + Z_R(x') = 0, \tag{1}$$

where Z_L and Z_R are the input impedances to the left and right of the terminals of the slot (reference point), respectively. In Figure 1b, L_s is the total stub length, S is the offset of the feed from the center, and d is as shown.

Note that because at the first resonance most of the current flows around the slot, and the slot resonates at that frequency, the first resonant frequency is anticipated to depend more on the outer circumference of the slot (and not on the mean circumference, as mentioned in [1]). The first resonant frequency is thus not affected by the length, L_s, of the stub.

However, for the second resonance, we can use transmission-line theory for the open-circuited transmission-line sections, and express Equation (1) as

$$jZ_0 \cot\left[\beta(\omega)d\right] + jZ_0 \cot\left[\beta(\omega)(L_s - d)\right] = 0, \quad (2)$$

or

$$\tan\left[\beta(\omega)L_s - \beta(\omega)d\right] = -\tan\left[\beta(\omega)d\right], \quad (3)$$

where Z_0 and $\beta(\omega)$ are the characteristic impedance and the propagation constant of the line. Note that the value of Z_0 does not affect the resonance condition, since all Z_0 terms cancel out in Equation (2). The equality in Equation (3) holds only when

$$\beta(\omega)L_s = n\pi, \; n = 1,2,3,...N. \quad (4)$$

This can be simplified to lead to

$$L_s = \frac{n\lambda_g}{2}, \; n = 1,2,3,...,N, \quad (5)$$

where λ_g is the guided wavelength of the coplanar waveguide line at the desired second resonant frequency, and n is a natural number. For $n = 1$, the condition in Equation (5) says that in addition to the first resonant frequency, f_1, an off-center-fed coplanar folded-slot antenna will also resonate at f_2 when the length, L_s, is adjusted to be $\lambda_g/2$ at that desired frequency f_2. Therefore, if Equation (5) for the length of the stub is satisfied, the equivalent circuit will resonate. When f_2 is close to f_1, the broadband mode is achieved. When f_2 is far from f_1, the dual-band mode is achieved. Since f_1 depends on the outer circumference of the slot, f_1 does not change by off-centering the feed or by changing L_s.

To verify the above derivation, four prototypes were designed based on the 2.4 GHz reference antenna, by shifting its feed line by S, as shown in Figure 1b. Shifting the feed maintains the good matching at f_1. According to Equation (5), L_s was made a half-wavelength at 3, 4, 4.5, and 5.25 GHz to achieve the second resonance at these frequencies. The feed line could also be made a half-wavelength long at f_2, and it would maintain its characteristic impedance of 50 Ω at both frequencies. All dimensions for each antenna are listed in Table 1.

The simulated return loss for all designs is shown in Figure 2. Good agreement was observed between the second resonant frequencies calculated from Equation (5) and the frequencies obtained using full-wave simulations [22]. Figure 2 also showed that f_1 is practically independent of L_s, which validated the use of the *outer* circumference for the calculation of the first resonance of the coplanar folded-slot antenna. Only in the broadband design was f_1 shifted slightly, from 2.4 to 2.5 GHz (a 4% shift), which appeared to be due to the over-coupling of the 2.4 and 3 GHz resonances, which are relatively close to each other. Table 2 shows that Equation (5) yielded less than 2% deviation between the calculated and simulated second resonant frequencies.

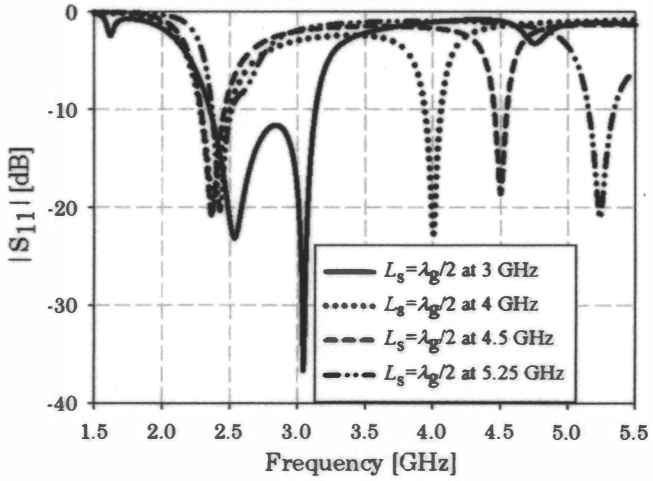

Figure 2. The simulated return-loss response of different broadband (3 GHz) and dual-band (4, 4.5, and 5.25 GHz) coplanar folded-slot antennas.

Table 1. The dimensions of the broadband and dual-band coplanar folded-slot antennas (in mm) (the first resonance for all designs was at 2.4 GHz).

Dimension	$f_2 = 3$ GHz	$f_2 = 4$ GHz	$f_2 = 4.5$ GHz	$f_2 = 5.25$ GHz
L_g	55	55	55	55
W_g	44.3	37.8	35.2	30
L_p	44.5	44.5	44.5	44.5
W_p	2.06	2.36	2.36	2.5
L_s	35.6	27.1	24.1	20.4
W_s	0.35	0.35	0.35	0.35
W_a	1.5	1.8	1.8	1.8
W_f	3.1	3.1	3.1	3.1
g	0.21	0.21	0.21	0.21
L_f	35.6	27.1	24.1	20.4
S	2.14	1.62	1.45	1.63

Table 2. The calculated and simulated second resonant frequencies for the off-center-fed coplanar folded-slot antennas.

Calculated from Equation (5) [GHz]	Simulated (*IE3D*) [GHz]	|Deviation| [%]
3	3.05	1.67
4	4.01	0.25
4.5	4.49	0.22
5.25	5.26	0.19

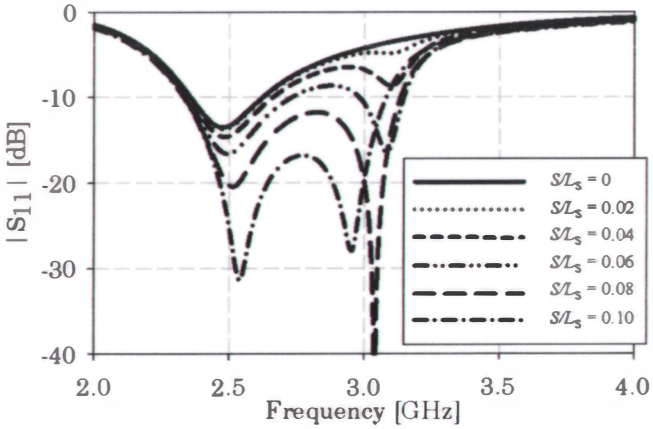

Figure 3. The simulated return-loss response of the off-center-fed broadband 2.4 GHz to 3 GHz coplanar folded-slot antenna for different S/L_s ratios of the feed offset to the stub length.

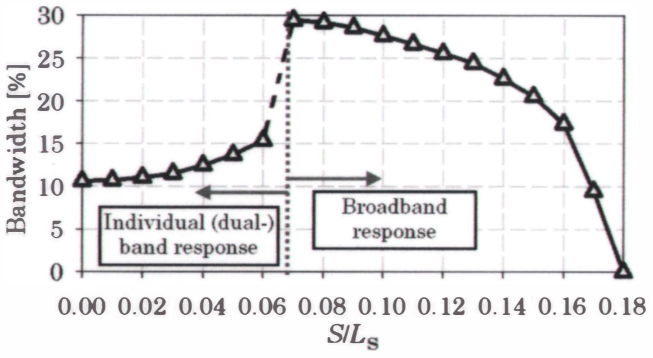

Figure 4. The simulated bandwidth of the broadband coplanar folded-slot antenna as a function of the ratio S/L_s for the 2.4 GHz and the 3 GHz antennas. The left-hand side bandwidth was the sum of the two individual bands. The first and second bands combined at $S/L_s \sim 0.07$ to the broadband coplanar folded-slot antenna.

2.2 Matching and Bandwidth Considerations

The previous derivation showed the condition for achieving the desired second resonant frequency for off-center-fed coplanar folded-slot antennas. However, it did not provide any information about the matching. The radiation mechanism is different at the first and second resonant frequencies.

At the first resonance, the antenna forms a resonant aperture, while at f_2 the stub resonates in a way similar to a $\lambda/2$ dipole, as will be shown in Section 3. Therefore, its input impedance at the second resonance depends upon the current distribution on the stub, and so it is a function of the feeding position. For this reason, it is practical to investigate the effect of the feed offset, *S*, on the return loss and bandwidth of the broadband and dual-band coplanar folded-slot antennas. The offset was studied in the form of the ratio S/L_s.

Figure 3 shows the return loss of the 2.4 GHz to 3 GHz broadband coplanar folded-slot antenna for different S/L_s ratios. At $S/L_s = 0$, we have the traditional single-resonant coplanar folded-slot antenna. As S/L_s increases, the second resonance is formed. The S/L_s ratio affects the matching of the second resonance, which couples with the first resonance which is nearby, and results in some over-coupling and a small shift of the first resonant frequency, from 2.4 to 2.5 GHz. At $S/L_s = 0.07$ – which means that *S* is equal to 0.07 of a half-wavelength ($\lambda_g/2$) at f_2 – the two resonances merge, and the broadband operation begins. The bandwidth obtained is then almost ~30%. This broadband mode persists up until $S/L_s = 0.16$, and vanishes beyond this ratio. The bandwidth as a function of S/L_s is shown in Figure 4. For $S/L_s \le 0.06$, the bandwidth shown is the sum of the two individual-band bandwidths for $|S_{11}| < -10$ dB at $Z_{in} = 50\,\Omega$, since the antenna has a single-band performance, or its second resonance is not yet well matched.

Similar parametric studies were made for the dual-band coplanar folded-slot antennas at 4, 4.5, and 5.25 GHz. For these antennas, the second resonance occurred far from the first (2.4 GHz), so their performance was always dual-band (i.e., no broadband mode appeared). Results for a practical dual-band coplanar folded-slot antenna at 2.4 GHz and 5.25 GHz for WLAN applications are in Figure 5. However, all three designs provided similar responses. Notice how the S/L_s ratio affects only the matching and bandwidth of the second resonance, and not of the first.

This tuning of the second resonance with S/L_s allows the matching of the stub of dual-band coplanar folded-slot antennas at impedances other than 50 Ω (e.g. 25 Ω, 75 Ω, 100 Ω, etc.), by offsetting the feed line at different S/L_s ratios. This can be seen in the Smith charts of Figure 6, which show the matching at each fre-

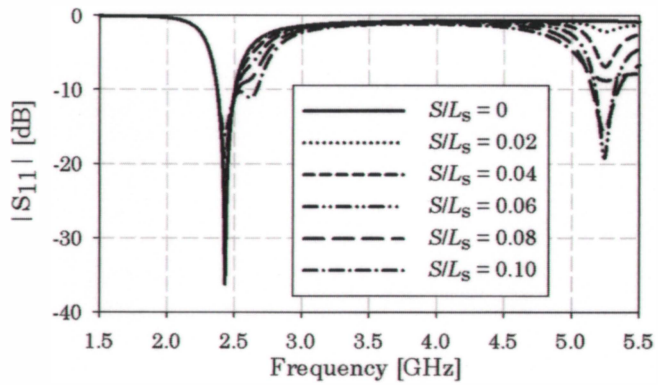

Figure 5. The simulated return loss of the dual-band coplanar folded-slot antenna with $f_1 = 2.4$ GHz and $f_2 = 5.25$ GHz for various S/L_s ratios. The first resonance remained unchanged while good matching was obtained at the second resonance.

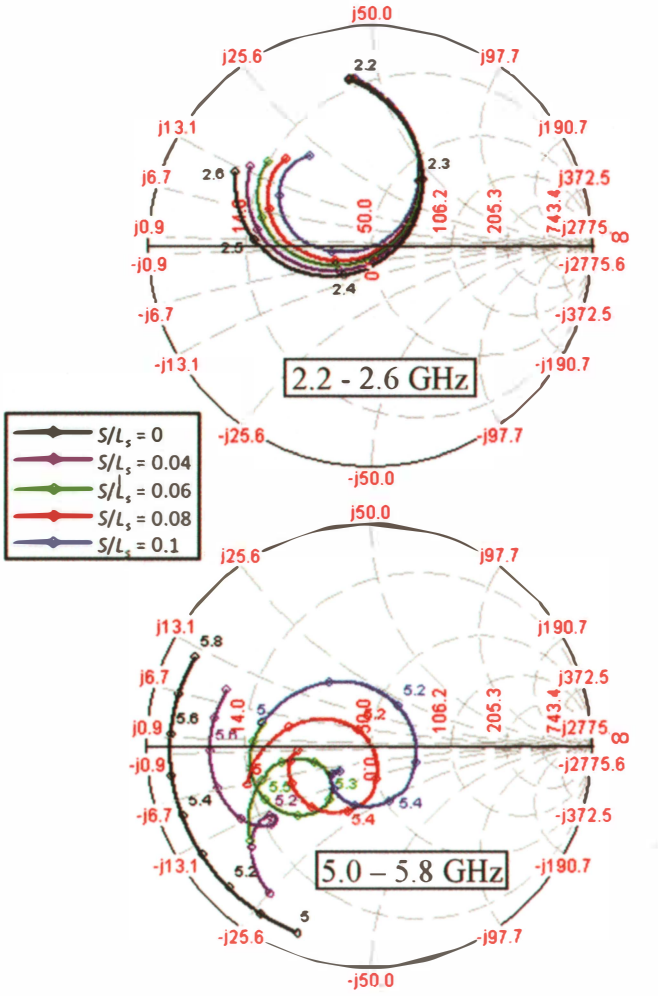

Figure 6. The impedance matching of the 2.4 GHz and 5.25 GHz dual-band antenna for various feed offsets. The input impedance of the 2.4 GHz resonance remained constant for all S/L_s ratios, while at 5.25 GHz, it increased rapidly with S/L_s.

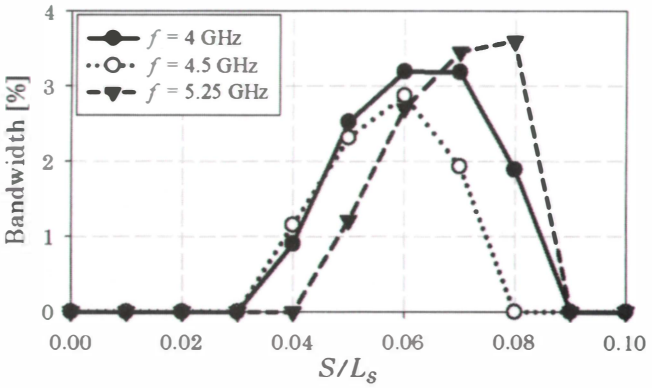

Figure 7. The simulated bandwidth of the second band of the dual-band designs as a function of the ratio S/L_s. The maximum bandwidth is typically obtained for values around $S/L_s \sim 0.07$.

quency (2.4 GHz and 5.25 GHz) as the feed was shifted for the dual-band design. Note that if an impedance other than 50 Ω is needed by a specific application, the antenna engineer may also need to match the first resonance of the antenna to that impedance value, as well.

The relationship of the bandwidth of the second resonance to the S/L_s ratio for the 4, 4.5, and 5.25 GHz antennas is summarized in Figure 7. It was shown that most (if not all) dual-band coplanar folded-slot antennas have good return losses and bandwidths at the second band when $0.04 \le S/L_s \le 0.09$, with the maximum values observed at ~0.07.

3. Broadband Prototype, Design, and Results

For a proof-of-concept, the presented methodology was first applied to design a broadband coplanar folded-slot antenna with a bandwidth of 2.4 GHz to 3 GHz. The single-band 2.4 GHz coplanar folded-slot antenna design was modified by first making the slot's *outer* circumference, P, close to one wavelength at f_1. More precisely, in our case, for an $\varepsilon_{r\_eff} = 1.76$, the perimeter should be $P = 2(W_p + W_a) = \lambda_g = 94$ mm. This design step was important, as it differed from what was mentioned in [1] for single-band coplanar folded-slot antennas, where it was stated that the *mean* slot perimeter should be λ_g. The length of the stub located inside the slot was then made equal to a half-wavelength at f_2 as given from Equation (5). The length of the 50 Ω coplanar waveguide feeding line was also made the same length. Next, an appropriate feed offset, S, was selected with respect to the length of the stub from Figure 4. If needed, W_a could have been adjusted to better match the antenna at f_1 [11]. All design dimensions are listed in the second column of Table 2.

A ratio of $S/L_s = 0.07$ was chosen, and the antenna was fabricated and measured. Its measured return loss (Figure 8) showed the two resonances as being at 2.55 GHz and 3.1 GHz, indicating a reasonable ~2% frequency shift from the simulations, and a 6% deviation from the 2.4 GHz, due to the aforementioned

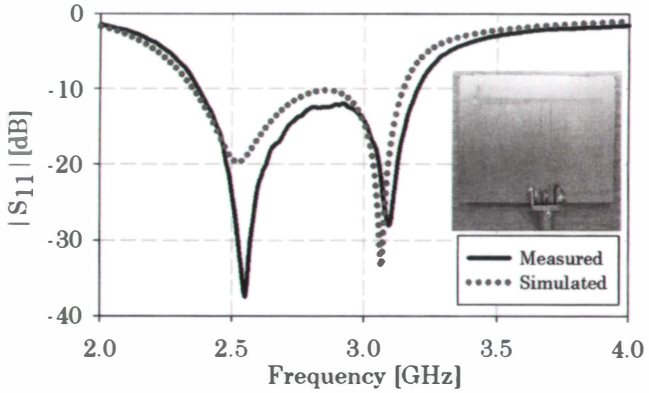

Figure 8. The simulated and measured return-loss responses of the 2.4 GHz to 3 GHz broadband coplanar folded-slot antenna. The measured bandwidth was 29.6%. The inset shows a photo of the fabricated broadband coplanar folded-slot antenna.

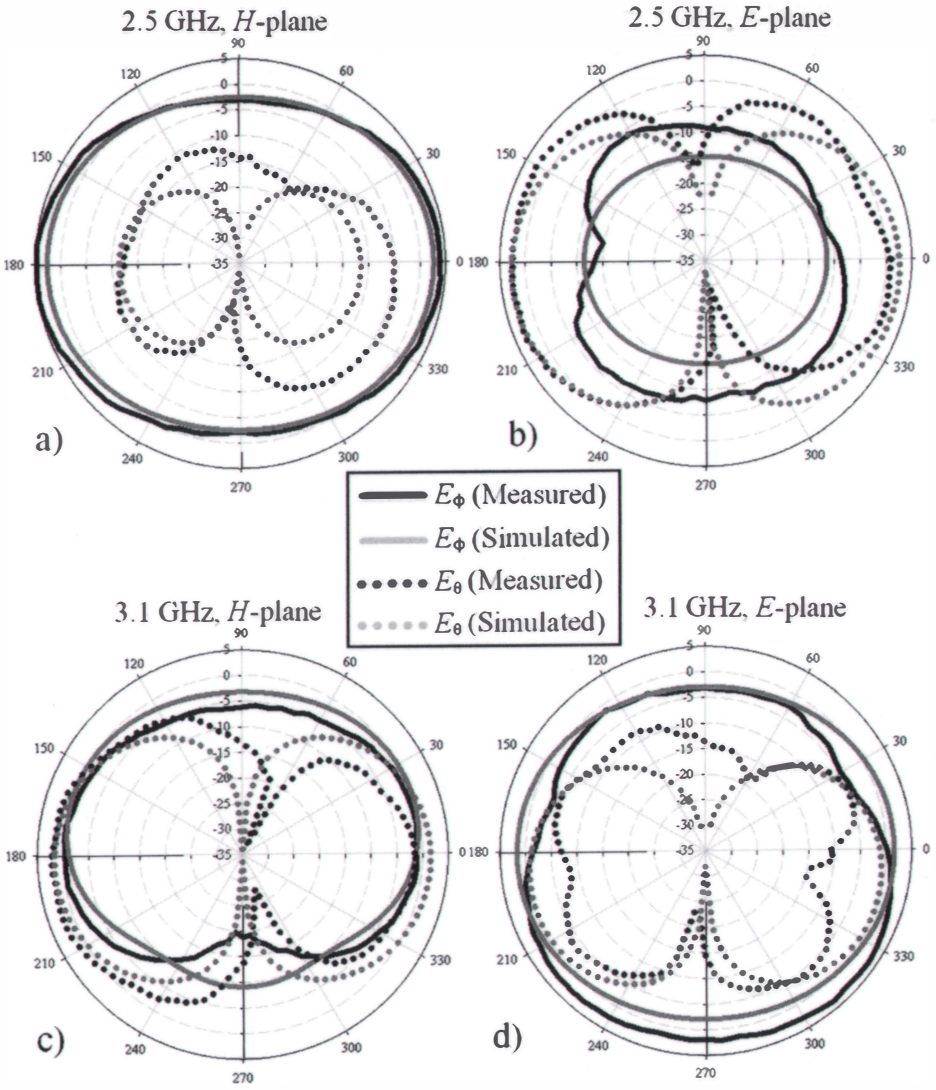

Figure 9. The simulated and measured radiation patterns of the broadband coplanar folded-slot antenna. Left: *H* plane, $\varphi = 0°$; right: *E* plane, $\varphi = 90°$; (a), (b): 2.5 GHz; (c), (d): 3.1 GHz.

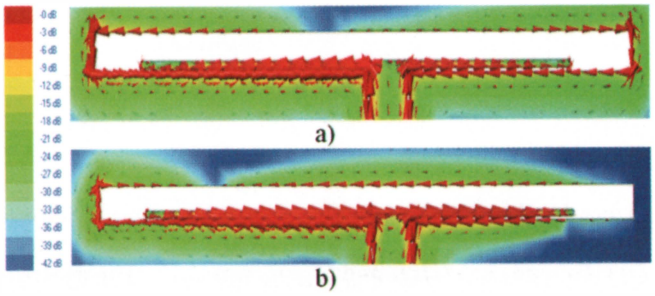

Figure 10. The simulated vector current distribution of the broadband coplanar folded-slot antenna at (a) 2.5 GHz and (b) 3.1 GHz.

over-coupling. The measured bandwidth was 29.6%, centered at 2.785 GHz. A photo of the fabricated prototype is also shown in Figure 8.

The radiation patterns of the antenna were measured in the custom-built anechoic chamber at SDSM&T, and were compared to the simulations, in Figure 9. At 2.5 GHz, the *H*-plane (*x-z* plane, $\varphi = 0°$) and *E*-plane (*y-z*, $\varphi = 90°$) patterns were typical of a folded-slot antenna, with a near-omnidirectional *H* plane, and two nulls in the *E* plane. The maximum measured gain was 4.8 dBi at 2.5 GHz, while at 3.1 GHz the gain was 3.5 dBi, a half dB higher than the simulated value, and significantly higher than the gain of a wire dipole antenna.

Note that for coplanar folded-slot antennas, the co-pol pattern in the *H* plane is the E_φ pattern, and in the *E* plane it is the E_θ pattern, while the cross-pol patterns are E_θ and E_φ, respectively. The cross-pol levels (E_θ in the *H* plane, and E_φ in the *E* plane) were relatively high at 3.1 GHz, since these were the major radiating fields at the second resonance. The reason for this can be understood by studying the average current density around the slot and on the stub at 2.5 GHz and 3.1 GHz, which is shown in Figure 10. At 2.5 GHz (Figure 10a), the current had high density around the outer circumference of the slot that resonates. Notice that the current vectors on the stub flowed in opposite directions in each arm. On the other hand, at 3.1 GHz, most of the current was concentrated on the stub and on its adjacent part of the coplanar waveguide ground, while it all flowed in one direction along the stub. This current distribution on the stub resembled that of a $\lambda/2$ dipole, and was responsible for strengthening the cross-pol com-

ponent of the radiation patterns at f_2. In other words, while the radiation at 2.5 GHz appeared to originate from a magnetic conducting surface, the radiation at 3.1 GHz originated from an electric conductor, which gave it a perpendicular polarization. This is as described by Booker's extension of Babinet's principle onto antennas to account for polarization [23].

4. Dual-Band Prototype, Design, and Results

To complete this study, the same methodology of Section 2 was also applied to the design of a dual-band coplanar folded-slot antenna, with f_2 far from f_1. The frequencies of 2.4 GHz and 5.25 GHz were arbitrarily chosen as a proof-of-concept of a conformal single-plane coplanar folded-slot antenna suitable for WLAN applications. Using Figure 7, a ratio of $S/L_x = 0.08$ was selected for sufficient bandwidth at f_2. The design steps were the same as in Section 3, and the antenna dimensions are listed in the fifth column of Table 1.

The antenna was fabricated and measured. The return loss, in Figure 11, showed good agreement between measurements and simulations, with less than 3% deviation.

A summary of the measured and simulated results in terms of the resonant frequencies and fractional bandwidths for both the broadband and dual-band antennas is shown in Table 3.

The radiation patterns are shown in Figure 12. The maximum measured gain at 2.4 GHz was 4.4 dBi, and at 5.25 GHz it was 1.2 dBi. At all frequencies, the measurements were close to the simulations. This antenna also had higher cross-pol at f_2, for the same reason as the broadband antenna. At f_2, the current flowed in one direction on the stub and radiated in the cross polarization. This current distribution is similar on most (if not all) off-centered broadband and dual-band coplanar folded-slot antennas, since they have the same electrical dimensions for the slot (at the first resonant frequency) and for the stub (at the second resonant frequency). The coplanar folded-slot antenna's radiating mechanisms for each band are therefore uncoupled.

4. Discussion and Conclusions

A unified approach was presented for achieving both broadband and dual-band coplanar folded-slot antenna designs by offsetting the antenna's feed line. A derivation for accurately obtaining the second resonant frequency was presented. The off-centered feed makes the antenna resonate at a second resonant frequency, f_2, (without significantly affecting the first resonance at f_1) when the length of the stub inside the slot is half a guided wavelength, $\lambda_g/2$, at that second resonant frequency. Broadband performance is obtained when f_2 is near f_1, while the dual-band mode is achieved when f_2 is far from f_1. The design guidelines covered a span of applications in the 2.4 GHz to 5.25 GHz range, with various bands and bandwidths.

Two proof-of-concept prototypes (one broadband and one dual-band) were designed using the proposed method, and were fabricated and measured. The broadband coplanar folded-slot antenna had a maximum measured bandwidth of 29.6%, while the dual-band antenna was made with a frequency ratio $f_2/f_1 = 2.18$. Both antennas exhibited the performance that was predicted by the calculations and the simulations with good accuracy. Minimal frequency shifts were observed, while the bandwidths and patterns of all antennas were as anticipated.

The proposed design procedure can be used at other frequencies, with other f_2/f_1 frequency ratios. Antenna prototypes at 4 GHz and 4.5 GHz were also fabricated, and their measurements (not shown for brevity) verified the presented calculations and simulations. In addition, the same design procedure can be followed to match asymmetric coplanar folded-slot antennas at other impedances by matching the antenna first at the first band, f_1. However, note that significantly higher f_2/f_1 values (e.g., above three) may be affected by the radiation from the third harmonic of f_1.

A summary of the design procedure for broadband and dual-band coplanar folded-slot antennas follows:

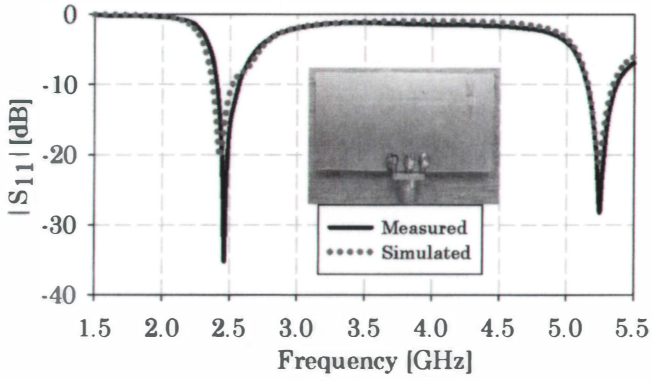

Figure 11. The simulated and measured return loss of the dual-band coplanar folded-slot antenna. The antenna resonated at 2.4 GHz and 5.25 GHz, and f_2/f_1 was 2.18. The measured return losses at 5.15 GHz and 5.35 GHz were 10.01 dB and 11.07 dB, respectively. The inset shows a photo of the fabricated dual-band coplanar folded-slot antenna.

Table 3. The resonant frequencies and a bandwidth summary for the broadband and dual-band coplanar folded-slot antennas.

Design	Measured (Simulated)			
	f_1 [GHz]	f_2 [GHz]	f_1 BW [%]	f_2 BW [%]
Broadband	2.55 (2.51)	3.09 (3.06)	29.7 (27.8)	
Dual-Band	2.47 (2.4)	5.25 (5.26)	6.2 (5.7)	4.1 (3.6)

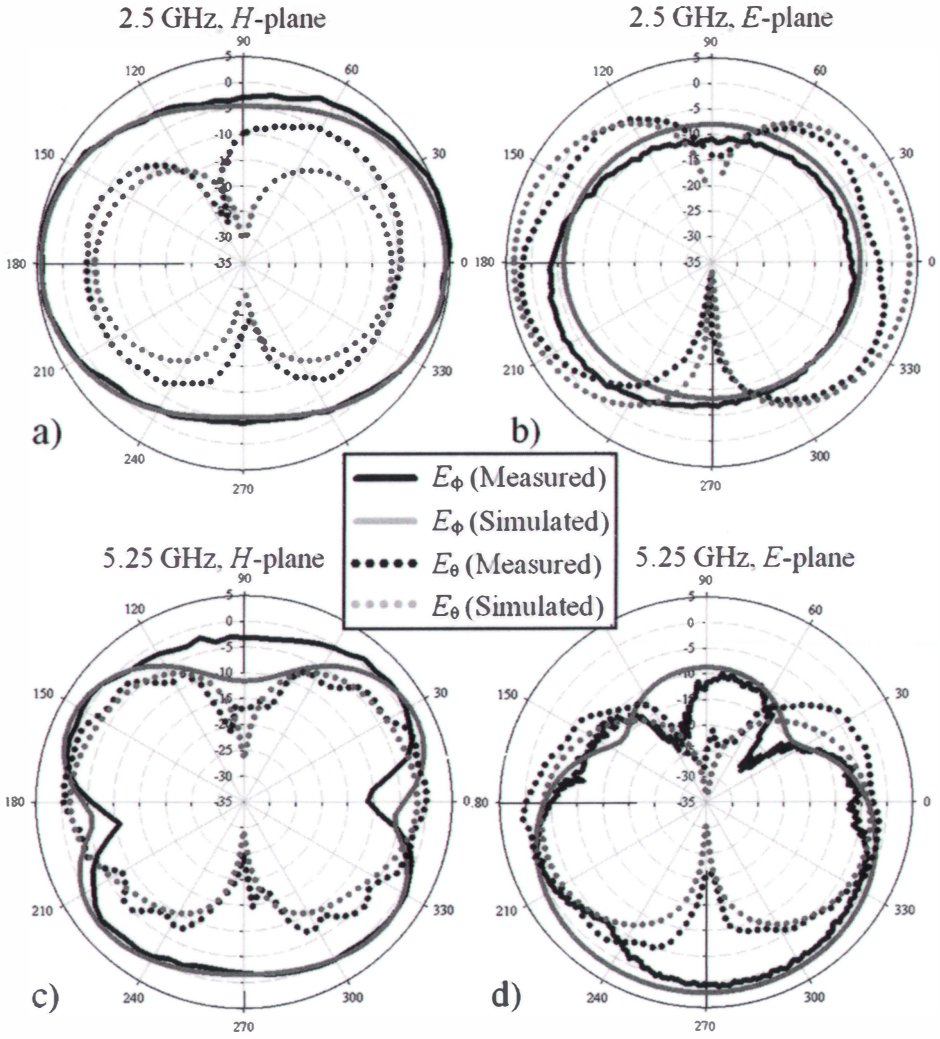

Figure 12. The simulated and measured radiation patterns of the dual-band coplanar folded-slot antenna. *H* plane, $\varphi = 0°$; right: *E* plane, $\varphi = 90°$; (a), (b): 2.5 GHz; (c), (d): 5.25 GHz.

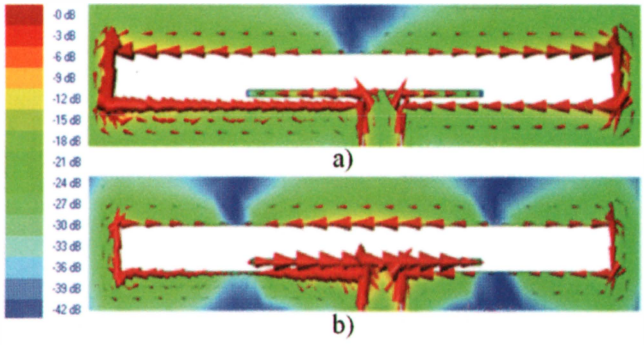

Figure 13. The simulated vector current distribution of the WLAN dual-band coplanar folded-slot antenna at (a) 2.4 GHz and (b) 5.25 GHz.

1. Design and match a single-band, coplanar folded-slot antenna that resonates at the lower frequency, f_1, following the design methodology and matching technique discussed in [1, 11] and mentioned briefly in Section 2. Modify the *outer* circumference of the slot to be equal to λ_g at f_1.

2. Make the length of the stub located inside the slot equal to a half-wavelength ($\lambda_g/2$) at f_2, as given from Equation (5).

3. Make the length of the 50 Ω coplanar waveguide feeding line equal to half a wavelength ($\lambda_g/2$) at f_2.

4. Select an appropriate feed offset, *S*, with respect to the length of the stub from Figure 4 for the broadband mode, or from Figure 7 for the dual-band mode.

5. If needed, adjust the dimension W_a to better match the antenna.

5. Acknowledgments

This work was supported in part by the Department of Defense, Army Research Office, Grant No. W911NF-09-1-0277; by the National Science Foundation, Grant No. 0824034; by National Science Foundation/EPSCoR Grant No. 0903804; and by NASA under Cooperative Agreement NNX07AL04A.

6. References

1. T. M. Weller, L. P. B. Katehi and G. M. Rebeiz, "Single and Double Folded-Slot Antennas on Semi-Infinite Substrates," *IEEE Trans. on Antennas and Propagation*, **AP-43**, 12, December 1995, pp. 1423-1428.

2. J. Papapolymerou, C. Schwartzlow and G. Ponchak "A Folded-Slot Antenna on Low Resistivity Si Substrate with a Polyimide Interface Layer for Wireless Circuits," Topical Meeting on Silicon Monolithic Integrated Circuits in RF Systems 2001, September 12-14, 2001, pp. 215-218.

3. H. S. Tsai, and R. A. York, "FDTD Analysis of CPW-Fed Folded-Slot and Multiple-Slot Antennas on Thin Substrates," *IEEE Transactions on Antennas and Propagation*, **AP-44**, 2, February 1996, pp. 217-226.

4. S. V. Robertson, N. I. Dib, G. Yang, and L. P. Katehi, "A Folded Slot Antenna for Planar Quasi-Optical Mixer Applications," 1993 IEEE International Symposium on Antennas and Propagation *Digest*, **2**, pp. 600-603.

5. H. S. Tsai, M. J. W. Todwell, and R. A. York, "Planar Amplifier Array with Improved Bandwidth Using Folded Slot," *IEEE Microwave and Guided Wave Letters*, **4**, 4, April 1994, pp. 112-114.

6. X. H. Yang and W. W. Zhang, "Coplanar Waveguide Antenna Arrays for MIC/MMIC at Millimeter Wave Frequencies," *Electronics Letters*, **26**, 18, August 1990, pp. 1464-1465.

7. M. C. Scardelletti, A. A. Omar, and N. Dib, "Planar and Cylindrical CPW Fed Dual Frequency Folded Slot Antennas," 2006 IEEE International Symposium on Antennas and Propagation *Digest*, Albuquerque, NM, pp. 4273-4276.

8. M. C. Scardelletti, J. L. Jordan, and G. E. Ponchak, "Temperature Dependency (25°C-400°C) of a Planar Folded Slot Antenna on Alumina Substrate," *IEEE Antennas and Wireless Propagation Letters*, **7**, 4, 2008, pp. 489-492.

9. A. M. Castro-Vilaro and R. A. Rodriguez-Sòlis, "Tunable Folded-Slot Antenna with Thin Film Ferroelectric Material," 2003 IEEE International Symposium on Antennas and Propagation *Digest*, June 2003, pp. 549-552.

10. D. E. Anagnostou and A. A. Gheethan, "A Coplanar Reconfigurable Folded Slot Antenna Without Bias Network for WLAN Applications," *IEEE Antennas and Wireless Propagation Letters*, **8**, 2009, pp. 1057-1060.

11. N. Lopez-Rivera, and R. A. Rodriguez-Solis, "Impedance Matching Technique for Microwave Folded Slot Antennas," 2002 IEEE International Symposium on Antennas and Propagation *Digest*, **3**, 2002, pp. 450-453.

12. R. Usaha and M. Ali, "Design of Broadband Modified Folded Slot Antennas for C-Band Wireless Applications," IEEE Topical Conference on Wireless Communication Technology, 2003, October 15-17, 2003, pp. 150-151.

13. A. A. Omar, M. C. Scardelletti, Z. M. Hejazi, and N. Dib, "Design and Measurement of Self-Matched Dual-Frequency Coplanar Waveguide-Fed-Slot Antennas," *IEEE Transactions on Antennas and Propagation*, **AP-55**, 1, January 2007, pp. 223-226.

14. D. Llorens, P. Otero, and C. Camacho-Penalosa, "Dual-Band, Single CPW Port, Planar-Slot Antenna," *IEEE Transactions on Antennas and Propagation*, **AP-51**, 1, January 2003, pp. 137-139.

15. S. D. Targonski, R. B. Waterhouse, and D. M. Pozar, "Design of Wide-Band Aperture-Stacked Patch Microstrip Antennas," *IEEE Transactions on Antennas and Propagation*, **AP-46**, 9, September 1998, pp. 1245-1251.

16. N. Behdad and K. Sarabandi, "A Wideband Slot Antenna Design Employing a Fictitious Short Circuit Concept," *IEEE Transactions on Antennas and Propagation*, **AP-53**, January 2005, pp. 475-482.

17. Available from Rogers Corporation, http://www.rogerscorp.com, 2009.

18. K. C. Gupta, R. Garg, I. Bahl, and P. Bhartia, *Microstrip Lines and Slotlines*, Norwood, MA, Artech House, 1996, Chapter 7, pp. 441-443.

19. M. Naghed and I. Wolff, "Equivalent Capacitances of Coplanar Waveguide Discontinuities and Interdigitated Capacitors Using a Three-Dimensional Finite Difference Method," *IEEE Transactions on Microwave Theory and Techniques*, **38**, 12, December 1990, pp. 1808-1815.

20. C. Balanis, *Advanced Engineering Electromagnetics*, New York, Wiley, 1989, Chapter 8, pp. 410-413.

21. D. Peroulis, K. Sarabandi and L. P. B. Katehi, "Design of Reconfigurable Slot Antennas," *IEEE Transactions on Antennas and Propagation*, **AP-53**, 2, February 2005, pp. 645-654.

22. *IE3D*, Zeland Software Inc., 2009; http://www.zeland.com.

23. H. G. Booker, "Slot Aerials and their Relation to Complementary Wire Aerials," *Proceedings of the IEE*, **90**, Pt. IIIA, 4, 1946, pp. 620-629.

Introducing the Authors

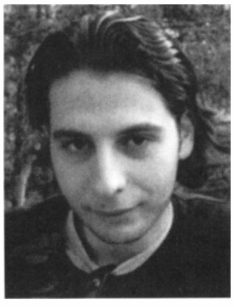

Ahmad A. Gheethan received the BSEE from the Jordan University of Science and Technology, Jordan, in 2007, and the MSEE from the South Dakota School of Mines and Technology, SD, in 2009. He is currently pursuing his PhD in Nanoscience and Nanoengineering at the South Dakota School of Mines and Technology. His research interests include the design and fabrication of antennas using direct-write deposition.

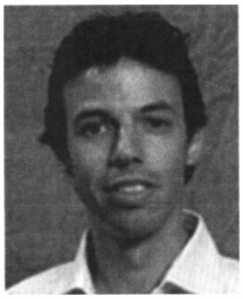

Dimitris E. Anagnostou received the BSEE from the Democritus University of Thrace, Greece, in 2000, and the MSEE and PhD degrees from the University of New Mexico in 2002 and 2005, respectively.

From 2005 to 2006, he was a Post-Doctoral Fellow at Georgia Institute of Technology, Atlanta, GA. Since 2007, he has been an Assistant Professor of Electrical and Computer Engineering at the South Dakota School of Mines and Technology, Rapid City, SD. He has published 55 peer-reviewed journal and conference papers. His current interests include analytical methods for antenna design, electrically small antennas, reconfigurable antennas and arrays, flexible arrays, metamaterial-inspired antennas and microwave circuits, antenna miniaturization, eco-friendly ("green" and paper) RF electronics, direct-write deposition, artificial dielectrics applications in electromagnetics, multifunctional antennas on solar cells, RF harvesters, wireless sensors, RF-MEMS, wireless signal propagation in tunnel environments, and microwave packaging.

Dr. Anagnostou received the 2010 IEEE John Kraus Antenna Award from the IEEE AP-S, and holds one patent on reconfigurable antennas. In 2006, he was awarded as a distinguished scientist living abroad by the Hellenic Ministry of Defense. He serves as an Associate Editor for the *IEEE Transactions on Antennas and Propagation* and the Springer *International Journal of Machine Learning and Cybernetics*. He has also been a member of the Technical Program Committee and session chair for the IEEE International Symposium on Antennas and Propagation. He has been a reviewer for 12 international publications. He has given two workshop presentations at the IEEE AP-S and IEEE MTT-S international symposia. Dr. Anagnostou is a member of Eta Kappa Nu, ASEE, and of the Technical Chamber of Greece.